

Resonant spin-flavor precession constraints on the neutrino parameters and the twisting structure of the solar magnetic fields from the solar neutrino data

S DEV¹, JYOTI DHAR SHARMA², U C PANDEY³, S P SUD¹ and B C CHAUHAN^{4,5}

¹Department of Physics, Himachal Pradesh University, Shimla 171 005, India

²Government College, Kotshera, Shimla 171 004, India

³IGNOU Regional Centre, Khanna 141 401, India

⁴Government College, Karsog Dist., Mandi 171 304, India

⁵Centro de Fisica das Intercooes Fundamentais, Instituto Superior Tecnico, Av. Rovisco Pais, 1096 Lisboa Codex, Portugal

MS received 27 December 2001; revised 6 January 2003; accepted 23 January 2003

Abstract. Resonant spin-flavor precession (RSFP) scenario with twisting solar magnetic fields has been confronted with the solar neutrino data from various ongoing experiments. The anticorrelation apparent in the Homestake solar neutrino data has been taken seriously to constrain $(\Delta m^2, \phi')$ parameter space and the twisting profiles of the magnetic field in the convective zone of the Sun. The twisting profiles, thus derived, have been used to calculate the variation of the neutrino detection rates with the solar magnetic activity for the Homestake, Super-Kamiokande and the gallium experiments. It is found that the presence of twisting reduces the degree of anticorrelation in all the solar neutrino experiments. However, the anticorrelation in the Homestake experiment is expected to be more pronounced in this scenario. Moreover, the anticorrelation of the solar neutrino flux emerging from the southern solar hemisphere is expected to be stronger than that for the neutrinos emerging from the northern solar hemispheres.

Keywords. Solar neutrino problem; resonant spin-flavor precession; twisting solar magnetic fields.

PACS Nos 26.65.+t; 13.40.Em; 14.60.Pq; 96.60.Hv

1. Introduction

The solar surface appears to be rich in magnetic activity. Almost all our knowledge of solar magnetic fields is based on surface measurements. The existence of the magnetic fields in the solar environment has been inferred from the observations of the Zeeman broadening of the spectral lines. The magnetic field certainly exists in the convective zone and may extend down to the core. The phenomena occurring on the solar surface are believed to be the outer manifestations of the inner dynamics which is responsible for the magnetic activity of the Sun. The main component of the solar magnetic field is toroidal with opposite polarities in the northern and the southern hemispheres. There are strong reasons to believe that the magnetic fields in the solar radiative interior are essentially permanent. However, the same

is not the case with the convective zone magnetic fields. The magnetic fields in the solar interior cannot be investigated with the earth-based experiments since the solar interior is opaque to the photons. The surface magnetic fields are within the reach of the terrestrial observations but these fields are not a simple extension of the long-lived inner magnetic fields. In fact, the convective and the radiative zone magnetic fields have entirely different origins. It is currently believed that the solar magnetic fields are generated by a dynamo process at the interface between the convective zone and the radiative core.

The solar magnetic activity shows some remarkable characteristic patterns. The periodic occurrence of the sunspots is one of the most familiar of these patterns. Another remarkable characteristic of the solar cycle is the periodic change in the orientation of the toroidal magnetic field lines in the convective zone which leads to the sunspot cycle. The toroidal magnetic fields are generated from the poloidal fields by the differential rotation of the Sun and the global convective current is responsible for the change in the orientation of the toroidal magnetic fields. The toroidal fields in the outer zone propagate towards the solar surface, spread and manifest as sunspots which eventually dissipate. One of the main goals of solar physics is to find a coherent explanation of the self-generating mechanism responsible for these periodic phenomena in the Sun. However, an exact solution of the relevant magnetohydrodynamic (MHD) equations governing the dynamics of the solar cycle is almost impossible. In the absence of an exact analytical treatment of the relevant MHD equations, numerical solutions have been attempted by prescribing the velocity fields of the differential rotation of the Sun and the global convection by introducing several adjustable parameters. Some of these computer simulations [1] reproduce the basic characteristics of the solar cycle to a remarkable degree of agreement. The magnetic flux tubes encircling the rotational axis of the Sun appear naturally in these simulations. The orientation of the toroidal magnetic field is reversed inside the convective zone. These reversed magnetic fields propagate towards the solar surface and manifest as sunspots which eventually dissipate.

At the sunspot maximum, the surface fields may reach 10^3 – 10^4 Gauss inside the spots and, then, extend far out in the solar atmosphere where they produce flares and prominences while at the sunspot minimum, the field falls below 10^2 Gauss. Below the surface to the bottom of the convective zone, the magnetic field could be large but the field response time due to plasma effects is of the order of 10^{10} years [2]. As a consequence, such a field, if it exists, will remain frozen over the entire life history of the Sun and would not be affected by the solar cycle. Besides this, little is known about the configuration and the strength of the inner solar magnetic fields. The observations are limited to the solar surface and the configuration and the strength of the inner solar magnetic fields have been sought to be extrapolated from the observations of the surface magnetic activity which is very complex and dynamical. In fact, the standard solar model (SSM), though, fairly successful in predicting the thermal and the nuclear evolution of the Sun, sheds little light on the solar magnetic activity. Our understanding of the solar magnetic activity is rather primitive and a generally accepted theory of the solar dynamo does not exist. The integration of the solar magnetic activity into the SSM, which governs the thermal and the nuclear evolution of the Sun, remains a distant dream.

Apart from the observed suppression of the solar neutrino flux, the Homestake data hint to an anticorrelation of the solar neutrino flux with the solar magnetic activity. Of course, the Kamiokande and the gallium experiments do not report any statistically significant anticorrelation but the statistics of all these experiments is too poor to rule out the anticor-

relation conclusively. The high statistics Super-Kamiokande, on the other hand, has been in operation for too short a period to confirm or disprove any anticorrelation. A majority of the statistical analyses [3] of the Homestake data using different statistical methods and different indicators of the solar magnetic activity hint to an anticorrelation and these studies indicate that the anticorrelation becomes stronger when a more local characteristic of the solar magnetic activity is chosen as indicator. Therefore, till such time as the issue of the anticorrelation of the solar neutrino flux with the solar magnetic activity is finally settled by the next generation high statistics solar neutrino experiments, the anticorrelation apparent in the Homestake data should be taken seriously. All the available solar neutrino data can be reconciled within the framework of resonant spin-flavor precession (RSFP) scenario [4] for a reasonable choice of neutrino parameters and solar magnetic field profiles [5]. Thus, at present, the RSFP of neutrinos remains as viable a solution of the solar neutrino problem as the fancied MSW mechanism. If future experiments confirm the anticorrelation of the solar neutrino flux with the solar magnetic activity, the RSFP will be overwhelmingly favoured since no other proposed solution can explain the anticorrelation.

Apart from the neutrino parameters, the RSFP of the neutrinos in the solar interior introduces additional astrophysical parameters into the analysis of the solar neutrino data. The examples of these parameters are the magnitude and the range of the magnetic fields in the radiation and the convection zones. The available astronomical data do not provide a reliable knowledge of these parameters. The solar neutrino fluxes observed in different solar neutrino experiments are expected to be sensitive to the magnetic field profiles in the solar interior which gives us an opportunity to discriminate between various possible solar magnetic field profiles from the solar neutrino data assuming the RSFP to be responsible for the depletion and the time-variation of the solar neutrino fluxes. Since most of the RSFP conversion occurs in the resonance region, a strong suppression of a particular component of the solar neutrino spectrum indicates a strong magnetic field in the resonance region in the solar interior for that particular component and vice versa. In this manner, one can map the magnetic field inside the solar interior. This principle was used by Chauhan, Pandey and Dev [5,6] to map the magnetic field distribution consistent with the different degrees of suppression observed in the Homestake, the Kamiokande and the gallium experiments.

An important implication of the solar dynamo is that the toroidal magnetic field receives twisting in the course of its time-evolution. The orientation of this twisting is likely to be opposite in the northern and the southern solar hemispheres. Computer simulations [1] of the relevant MHD equations governing the solar cycle are fairly successful in reproducing the basic characteristics of the solar cycle and the magnetic flux tubes encircling the axis of rotation of the Sun appear naturally in these simulations. The magnetic field around the circling tube is twisting but the twisting parameter is not uniquely determined. In this work, the RSFP in the presence of twisting magnetic fields has been confronted with the solar neutrino data to constrain the twisting parameter. In particular, the anticorrelation apparent in the Homestake data has been taken seriously to constrain the possible profiles of the solar magnetic fields.

2. Neutrino evolution in the twisting magnetic fields

We consider, for simplicity, two generations of Majorana neutrinos and their antiparticles with a transition magnetic moment $\mu_{\nu_e\nu_\mu}$ (μ for short) between them. We take the z -axis along the neutrino path and the x -axis along the axis of rotation of the Sun. Then, the

toroidal part of the magnetic field gives the x -component and the twisting part gives the y - and the z -components. The fields relevant to spin-flip are those transverse to the neutrino path and are parameterized as

$$Bx + iBy = B_{\perp} \exp(i\phi). \quad (1)$$

The significance of the phase ϕ , which is an example of the geometrical ‘Berry phase’ [7], for neutrino propagation in matter in the presence of the twisting magnetic fields was first realized by Vidal and Wudka [8]. Further investigations to examine the implications of this phase for neutrino propagation in magnetic fields twisting along the neutrino path were undertaken by Smirnov [9], Aneziris and Schechter [10] and Toshev [11]. Further consequences of twisting toroidal magnetic fields for solar neutrino fluxes have been extensively studied by Smirnov [12] and also by Akhmedov, Krastev and Smirnov [13]. Kubota *et al* [14] and Kubota, Kurimoto and Takasugi [15] have examined the implications of this phase for the possible seasonal variations of the solar neutrino flux. The possible consequences of this phase for the neutrino fluxes in the Sudbury neutrino observatory (SNO) and Borexino experiments have been investigated by Balantekin and Loreti [16]. This phenomenon has been further investigated by Toshev [11,17] using exact analytical methods in the adiabatic case and by Akhmedov, Krastev and Smirnov [18] using numerical methods in the nonadiabatic case. It has been realized that some important differences notwithstanding, the phenomenon of twisting magnetic fields has remarkable similarities with the Mikheyev–Smirnov–Wolfenstein (MSW) effect [12].

We define a basis with two-flavor Majorana neutrinos and their antiparticles, viz.

$$\psi = (v_{eL}, v_{\mu L}, \bar{v}_{eR}, \bar{v}_{\mu R}), \quad (2)$$

where the mixing between the two flavors is generated by a Majorana mass term. The inclusion of the τ -neutrinos into the analysis is rather straightforward. The time evolution of the neutrino flavor states ψ as the neutrinos propagate in the matter in the presence of transverse magnetic field twisting along the neutrino path is governed by a Schrödinger-like equation:

$$i \frac{d\psi}{dt} = H\psi, \quad (3)$$

where

$$H = \begin{pmatrix} H_{\nu} & B_{\perp} e^{-i\phi} M^{\dagger} \\ B_{\perp} e^{i\phi} M & H_{\bar{\nu}} \end{pmatrix}. \quad (4)$$

The phase angle ϕ defines the direction of the magnetic field B_{\perp} in a plane transverse to the neutrino momentum. One can perform a phase rotation to move into a reference frame which rotates with the same angular velocity as the transverse magnetic field [9] by defining

$$\psi = S\psi', \quad (5)$$

where S is a diagonal matrix given by

$$S = \text{diag}(e^{-i\phi/2}, e^{i\phi/2}, e^{-i\phi/2}, e^{i\phi/2}). \quad (6)$$

RSFP constraints on the neutrino parameters

The matrix S being diagonal, neutrino transition probabilities remain unchanged with the change in the frame of reference and the same notation for neutrino states can be retained. The net effect of phase rotation is that phase factors $e^{i\phi}$ in the potential matrix get eliminated but an additional factor of half of the time derivative of phase ($\phi'/2$) gets subtracted from the diagonal elements of the effective potential.

With this phase rotation, the 2×2 submatrices are now given by

$$H_V = \begin{pmatrix} \frac{\Delta m^2}{2E} \sin^2 \theta + a_e - \frac{\phi'}{2} & \frac{\Delta m^2}{4E} \sin 2\theta \\ \frac{\Delta m^2}{4E} \sin 2\theta & \frac{\Delta m^2}{2E} \cos^2 \theta + a_\mu - \frac{\phi'}{2} \end{pmatrix} \quad (7)$$

and

$$M = \begin{pmatrix} 0 & -\mu \\ \mu & 0 \end{pmatrix}. \quad (8)$$

The appearance of the additional term $-(\phi'/2)$ can be regarded as a modification of the effective density. Here θ is the mixing angle and Δm^2 is the mass squared difference between the two neutrino mass eigenstates and E is the neutrino energy. The 2×2 submatrix $H_{\bar{\nu}}$ can be obtained from H_V by the replacement: $(a_e, a_\mu, \phi') \rightarrow (-a_e, -a_\mu, -\phi')$ where the matter potentials a_e and a_μ for a neutral unpolarized medium are given by

$$\begin{aligned} a_e &= \frac{G_F}{\sqrt{2}}(2N_e - N_n), \\ a_\mu &= -\frac{G_F}{\sqrt{2}}N_n. \end{aligned} \quad (9)$$

The MSW transitions are not affected by the onset of twisting but the magnetic transitions get altered and the condition for $\nu_e \rightarrow \bar{\nu}_\mu$ resonance now becomes

$$G_F \sqrt{2}(N_n - N_e) - \phi' = \frac{\Delta m^2}{2E} \cos 2\theta. \quad (10)$$

An additional $\nu_\mu \rightarrow \bar{\nu}_e$ resonance is now possible for positive twisting rates ϕ' with the resonance condition given by

$$G_F \sqrt{2}(N_n - N_e) + \phi' = \frac{\Delta m^2}{2E} \cos 2\theta. \quad (11)$$

Henceforth, we will take neutrino mixing to be zero.

The evolution of probability amplitudes ($A_{L,R}$) for transitions between the left-handed and the right-handed neutrino states in a transverse magnetic field is governed by the following equations:

$$\begin{aligned} i \frac{dA_R}{dz} &= B_0 A_R(z) + \mu B_\perp e^{-i\phi} A_L(z), \\ i \frac{dA_L}{dz} &= \mu B_\perp e^{-i\phi} A_R(z) - B_0 A_L(z), \end{aligned} \quad (12)$$

where

$$B_0 = -\frac{G_F}{\sqrt{2}}(N_e - N_n) + \frac{\Delta m^2}{2E} \quad (13)$$

for Majorana neutrinos for which the RSFP transition is $\nu_{eL} \rightarrow \bar{\nu}_{\mu R}$. Here, $A_R(z)$ and $A_L(z)$ are the probability amplitudes for right-handed ($\bar{\nu}_{\mu R}$) and left-handed (ν_{eL}) neutrinos at a distance z respectively. The neutrinos have been considered to be ultrarelativistic. In a realistic situation, B_0, B_\perp and also the twist frequency ϕ are z -dependent. For the case, when B_0 and $\phi(z)$ are linear functions of z , the Landau–Zener type probability is given by [11]

$$P_{LZ}^{\text{lin}} = \exp\left(\frac{-2\pi\mu^2 B_\perp^2}{\left|\frac{d\phi'}{dz} - 2\frac{dB_0}{dz}\right|}\right) \quad (14)$$

and the averaged survival probability for the left-handed electronic neutrinos is given by

$$\bar{P}_{\text{surv}} = \frac{1}{2} + \left(\frac{1}{2} - P_{LZ}^{\text{lin}}\right) \cos 2\theta_i \cos 2\theta_f. \quad (15)$$

Pulido [19] has shown that the Landau–Zener approximation which assumes a linearly decreasing matter density in the vicinity of the resonance works fairly well in the Sun. If we ignore the energy range and the production zone distribution, we get $\cos 2\theta_i \sim +1$ and $\cos 2\theta_f \sim -1$ which implies that

$$P_{\text{surv}} = P_{LZ} = \exp\left(\frac{-2\pi\mu^2 B_\perp^2}{\left|\frac{d\phi'}{dz} - 2\frac{dB_0}{dz}\right|}\right). \quad (16)$$

Moreover, because of the resonant character of the phenomenon and assuming $\phi'(z)$ to be an arbitrary smooth function, one can approximate it with a linear function in the vicinity of the resonance. Thus, because of the resonant character of the phenomenon under consideration, the results obtained in the linear case are also valid for arbitrary smoothly varying B_0 and ϕ' . However, the derivatives are, now, to be evaluated at the resonance point so that the survival probability is now given by [11,17]

$$P_{\text{surv}} = P_{LZ} = \exp\left(\frac{-2\pi\mu^2 B_\perp^2}{\left|\frac{d\phi'}{dz} - 2\frac{dB_0}{dz}\right|_{\text{res}}}\right), \quad (17)$$

where the resonance points are given by

$$\phi' - 2B_0 = 0. \quad (18)$$

3. RSFP constraints on the twisting profiles of the solar magnetic fields from the solar neutrino data

The first generation solar neutrino experiments, because of their poor statistics, are not in a position to conclusively confirm or disprove anticorrelation of solar neutrino flux with

the solar magnetic activity. However, a majority of statistical studies of the solar neutrino data from Homestake, which has been in operation for the longest period of time, favor a time-varying solar neutrino flux anticorrelated with solar magnetic activity. Thus, until such time as the issue of time-variations of the solar neutrino flux is finally settled by the next generation high statistics experiments, the anticorrelation apparent in the Homestake data must be taken seriously. Now, we wish to confront the anticorrelation apparent in the Homestake solar neutrino data with the resonant spin-flavor precession of neutrinos in the twisting solar magnetic fields. If the anticorrelation in the Homestake data is real, then both the boron and the beryllium neutrinos, comprising 78% and 22% of the neutrino signal in Homestake respectively, must experience time-varying magnetic fields in the solar convective zone.

From eq. (10), it is clear that a higher positive twist will push the $\nu_e \rightarrow \bar{\nu}_\mu$ resonance deeper into the Sun. One can determine the maximum possible twisting rate in the solar convective zone not in conflict with the anticorrelation observed in the Homestake by requiring the ${}^7\text{Be}$ neutrinos to undergo resonant spin-flavor conversion just at the bottom of the convective zone (BCZ), i.e.

$$G_{\text{F}}\sqrt{2}(N_e - N_n)|_{r=0.7} - \phi'_{\text{max}} = \frac{\Delta m^2}{2E} \Big|_{E=0.862 \text{ MeV}}, \quad (19)$$

where $r = z/R_s$. Any further increase in the twisting rate beyond ϕ'_{max} will decrease the effective density below the critical level required by the ${}^7\text{Be}$ neutrinos to undergo resonant spin-flavor conversion anywhere inside the convective zone of the Sun.

The minimum possible twisting rate in the convective zone of the Sun, not in conflict with the anticorrelation observed in the Homestake, can be determined by noting that the negative twisting leads to an increase in the effective density and the RSFP resonance is, accordingly, pushed outwards in the convective zone. The minimum possible twisting rate in the convective zone, not in conflict with the anticorrelation apparent in the Homestake data can, thus, be determined by requiring the ${}^8\text{B}$ neutrinos to undergo RSFP conversion just at the surface of the convective zone (SCZ), i.e.

$$G_{\text{F}}\sqrt{2}(N_e - N_n)|_{r=1} - \phi'_{\text{min}} = \frac{\Delta m^2}{2E} \Big|_{E=10 \text{ MeV}}. \quad (20)$$

Any further decrease in the twisting rate below ϕ'_{min} will increase the effective density above the critical level required by the ${}^8\text{B}$ neutrinos to undergo resonant spin-flavor conversion anywhere inside the Sun.

The low energy neutrinos, on the other hand, account for the dominant contribution to the neutrino signal in the gallium experiments which have not observed any statistically significant time-variations in the neutrino flux. As such, the low energy neutrinos are expected to undergo RSFP conversion within the radiation zone (i.e. between $r = 0.05$ to $r = 0.65$ where $r = z/R_s$) of the Sun where they experience magnetic fields constant in time and without any twisting. This, rather, simple restriction yields the following range of possible Δm^2 values

$$1.54 \times 10^{-8} \text{ eV}^2 < \Delta m^2 < 1.148 \times 10^{-5} \text{ eV}^2, \quad (21)$$

where the average energy of pp neutrinos has been taken to be 0.420 MeV. In the presence of twisting magnetic fields, the location of the RSFP resonance $\nu_e \rightarrow \bar{\nu}_\mu$ is given by

$$r_{\text{res}} = \left(\frac{z}{R_s} \right)_{\text{res}} = 0.09 \ln \left(\frac{1.42 \times 10^4}{\frac{\Delta m^2}{2E} (5.162 \times 10^{14}) + \phi'} \right), \quad (22)$$

where ϕ' is in rev/Rs. For $\Delta m^2 = 1.54 \times 10^{-8} \text{ eV}^2$ the RSFP resonance in the absence of twisting (i.e. $\phi' = 0$) for ${}^7\text{Be}$ neutrinos ($E = 0.862 \text{ MeV}$) and ${}^8\text{B}$ neutrinos ($E = 10 \text{ MeV}$) is located at

$$(r)_{{}^7\text{Be}}^{\text{res}} = 0.715,$$

and

$$(r)_{{}^8\text{B}}^{\text{res}} = 0.936. \quad (23)$$

As noted earlier, a positive twist will push these resonances deeper into the Sun and a maximum positive twist of 0.9253 rev/Rs is admissible if we do not wish to push the RSFP resonance for ${}^7\text{Be}$ neutrinos below the bottom of the convective zone (BCZ) (at $x = 0.7$) as required by the anticorrelation apparent in the Homestake where their contribution to the neutrino flux is about 22% of the total. On the other hand, a negative twist leads to an increase in the effective density as a result of which the RSFP resonance is pushed outwards. A negative twist of -0.2198 rev/Rs will eventually push the RSFP resonance for ${}^8\text{B}$ neutrinos right up to the surface of the convective zone (SCZ) and a higher negative twist ($\phi' < -0.2198 \text{ rev/Rs}$) implies the absence of the requisite effective density for ${}^8\text{B}$ neutrinos to undergo resonant spin-flavor conversion anywhere inside the Sun. This situation has been depicted in figure 1 where the lines of resonance for ${}^7\text{Be}$ and ${}^8\text{Be}$ neutrinos have been drawn on a $(\phi', G_F \sqrt{2}(N_e - N_n))$ plane for $\Delta m^2 = 1.54 \times 10^{-8} \text{ eV}^2$. It is clear from figure 1 that for this value of Δm^2 , both ${}^7\text{Be}$ and ${}^8\text{Be}$ neutrinos resonate within the convective zone in the presence of twisting magnetic fields with a maximum positive twisting rate of 0.9253 rev/Rs and a minimum twisting rate of 0.2198 rev/Rs. For $\Delta m^2 = 1.93 \times 10^{-8} \text{ eV}^2$, the RSFP resonance in the absence of twisting ($\phi' = 0$) is located at

$$(r)_{{}^8\text{B}}^{\text{res}} = 0.921 \quad (24)$$

for boron neutrinos and at

$$(r)_{{}^7\text{Be}}^{\text{res}} = 0.7 \quad (25)$$

for beryllium neutrinos. No positive twist is now admissible since a positive twist will push the RSFP resonance for ${}^7\text{Be}$ neutrinos below the bottom of the convective zone where the magnetic fields do not vary in time. A negatively twisted magnetic field, on the other hand, will push the RSFP resonance outwards and a negative twist beyond $\phi' = -0.29 \text{ rev/Rs}$ will make it impossible for ${}^8\text{B}$ neutrinos to undergo resonant spin-flavor precession anywhere inside the Sun. This situation has been depicted in figure 2 by drawing the lines of resonance for ${}^7\text{Be}$ and ${}^8\text{B}$ neutrinos on a $(\phi', G_F \sqrt{2}(N_e - N_n))$ plane for $\Delta m^2 = 1.93 \times 10^{-8} \text{ eV}^2$. For $\Delta m^2 > 1.93 \times 10^{-8} \text{ eV}^2$, there are no common values of ϕ' for which both the ${}^7\text{Be}$ and ${}^8\text{B}$ neutrinos undergo resonant spin-flavor conversion within the solar convective zone. The situation has been depicted in figure 3 for $\Delta m^2 = 3.0 \times 10^{-8} \text{ eV}^2$.

The allowed $(\phi', \Delta m^2)$ parameter space, consistent with the anticorrelation apparent in the Homestake solar neutrino data, has been depicted in figure 4.

For values of $\Delta m^2 > 1.93 \times 10^{-8} \text{ eV}^2$, no constant values of ϕ' will make both the ${}^7\text{Be}$ and ${}^8\text{B}$ neutrinos to undergo RSFP conversion within the solar convective zone. However,

RSFP constraints on the neutrino parameters

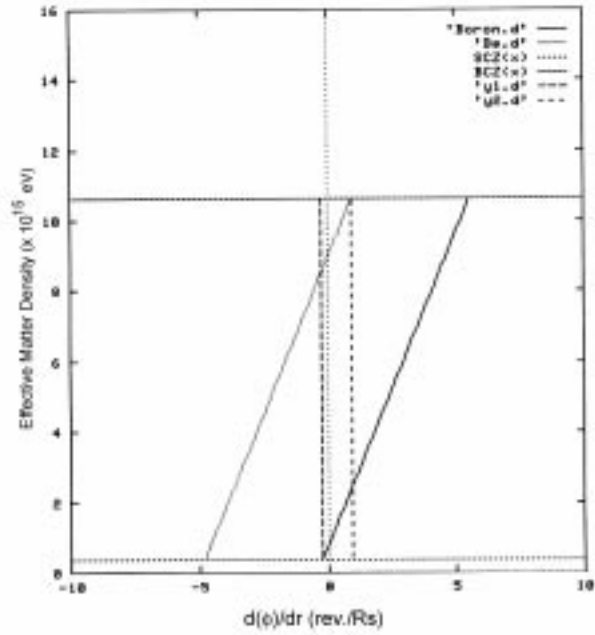


Figure 1. Lines of resonance for ${}^7\text{Be}$ and ${}^8\text{B}$ neutrinos on the $(\phi', G_F\sqrt{2}(N_e - N_n))$ plane for $\Delta m^2 = 1.54 \times 10^{-8} \text{ eV}^2$.

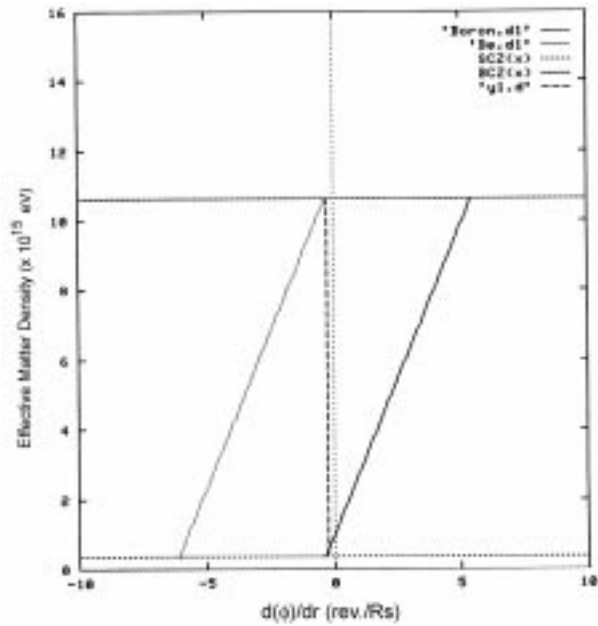


Figure 2. Lines of resonance for ${}^7\text{Be}$ and ${}^8\text{B}$ neutrinos on the $(\phi', G_F\sqrt{2}(N_e - N_n))$ plane for $\Delta m^2 = 1.93 \times 10^{-8} \text{ eV}^2$.

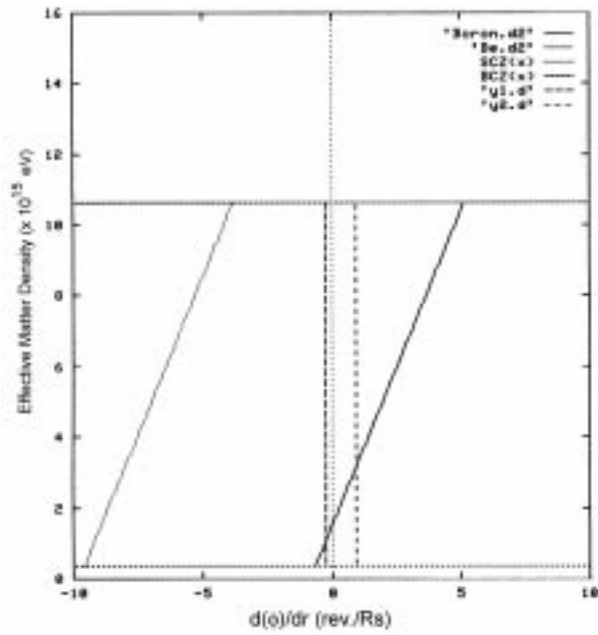


Figure 3. Lines of resonance for ${}^7\text{Be}$ and ${}^8\text{B}$ neutrinos on the $(\phi', G_F \sqrt{2}(N_e - N_n))$ plane for $\Delta m^2 = 3 \times 10^{-8} \text{ eV}^2$.

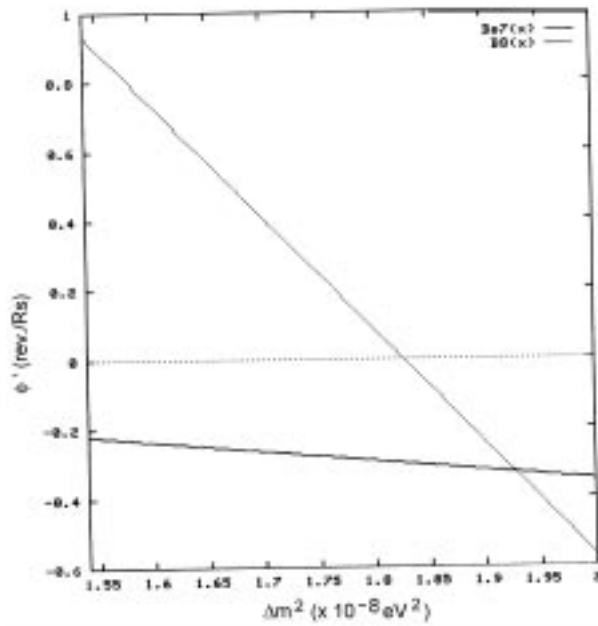


Figure 4. Allowed $(\Delta m^2, \phi')$ parameter space consistent with the anticorrelation apparent in the Homestake solar neutrino data.

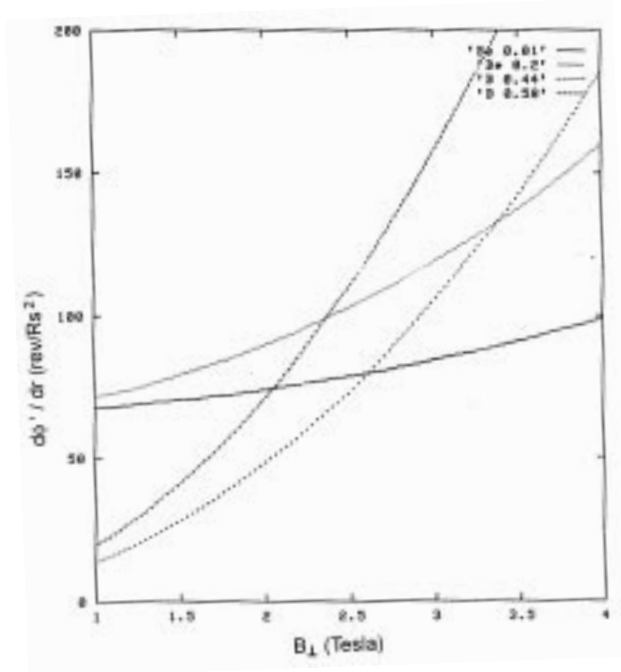


Figure 5. $(d\phi'/dr, B_{\perp})$ space consistent with the solar neutrino data.

for these values of Δm^2 , both the ${}^7\text{Be}$ and ${}^8\text{B}$ neutrinos could still undergo resonant spin-flavor conversion within the convective zone for magnetic fields with variable twisting.

One can determine the $(d\phi'/dr, B_{\perp})$ parameter space consistent with the solar neutrino data by making use of eq. (17) to draw constant probability curves for ${}^7\text{Be}$ and ${}^8\text{B}$ neutrinos which are expected to undergo RSFP conversion in the convective zone of the Sun. Because of the modulus in the denominator (eq. (17)), one obtains two sets of $(d\phi'/dr, B_{\perp})$ parameter space corresponding to the northern and the southern hemispheres of the Sun. The results have been shown in figure 5. It is interesting to note that very stringent limits are implied for the convective zone magnetic field. The survival probabilities for ${}^7\text{Be}$ and ${}^8\text{B}$ neutrinos have been taken to be in the following range [5]:

$$0 < P_{\text{Be}}^{\text{surv}} < 0.2, \quad 0.44 < P_{\text{B}}^{\text{surv}} < 0.58. \quad (26)$$

Now, we wish to determine the twisting rate profile of the convective zone magnetic field. Since most of the RSFP conversion occurs in the resonance region, one can determine the twisting rate at different locations of the resonance. To be more specific, let us consider that hemisphere of the Sun where the magnetic fields are positively twisted. We recall that for $\Delta m^2 = 1.54 \times 10^{-8} \text{ eV}^2$, the ${}^7\text{Be}$ resonance in the absence of twisting is located at

$$(r)_{7\text{Be}}^{\text{res}} = 0.714 \quad (27)$$

and a maximum positive twist of 0.9253 rev/Rs is admissible so that the ${}^7\text{Be}$ neutrinos resonate just at the bottom of the convective zone (at $r = 0.7$). Thus one can write a Taylor expansion for ϕ' around $r = 0.714$:

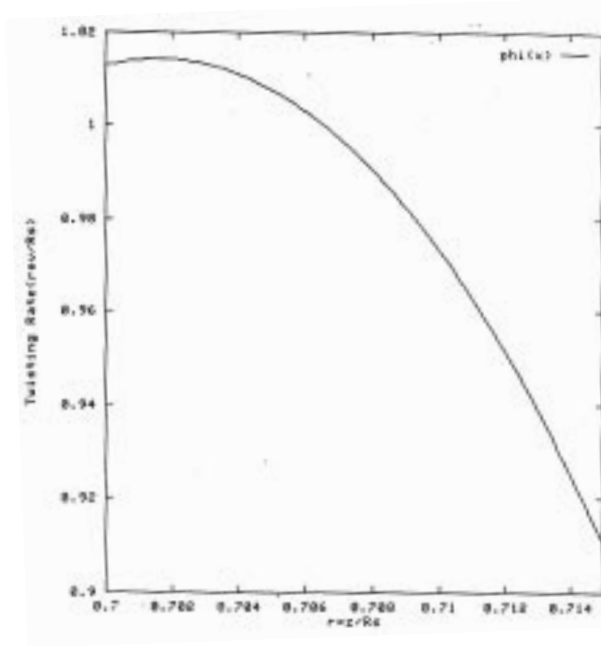


Figure 6. Twisting rate profile in the resonance region for ${}^7\text{Be}$ neutrinos.

$$\phi'(r) = \phi'(r = 0.714) + \left. \frac{d\phi'}{dr} \right|_{0.714} (r - 0.714) + \left. \frac{d^2\phi'}{dr^2} \right|_{0.714} \frac{(r - 0.714)^2}{2!} + \dots, \quad (28)$$

where the derivative $d\phi'/dr$ in the resonance region can be obtained by inverting eq. (17) and taking the appropriate sign as

$$\frac{d\phi'}{dr} = 15.811198 \times 10^4 \exp\left(\frac{-r}{0.09}\right) + 9.377949 \frac{B_{\perp}^2}{\ln P} \quad (29)$$

and substituting $P_{7\text{Be}}^{\text{surv}} = 0.20$ (95% C.L.). For the magnetic field, we adopt the Akhmedov distribution of the magnetic field given by

$$B_{\perp}(r) = \left\{ \begin{array}{ll} B_1 \left(\frac{\gamma}{r+\gamma}\right)^k, & 0 \leq r \leq 0.7 \text{ with } \gamma = 0.2, k = 2 \\ B_0 \left(1 - \left(\frac{r-0.7}{0.3}\right)^2\right), & 0.7 \leq r \leq 1 \end{array} \right\} \quad (30)$$

with $B_0 = 3.5T$ as dictated by the $(d\phi'/dr, B_{\perp})$ parameter space determined earlier. The resulting twisting profile has been shown in figure 6.

To determine the twisting profile of the negatively twisted magnetic fields in the other hemisphere, one must use the other equation obtained from eq. (17), viz.

$$\frac{d\phi'}{dr} = 15.811198 \times 10^4 \exp\left(\frac{-r}{0.09}\right) - 9.377949 \frac{B_{\perp}^2}{\ln P}. \quad (31)$$

RSFP constraints on the neutrino parameters

We recall that for $\Delta m^2 = 1.54 \times 10^{-8} \text{ eV}^2$, the RSFP resonance for ${}^8\text{B}$ neutrinos in the absence of twisting is located at $(r)_{\text{RSFP}}^{\text{res}} = 0.936$ and a negative twist higher than 0.2198 rev/Rs implies the absence of the requisite effective density for ${}^8\text{B}$ neutrinos to undergo RSFP conversion anywhere inside the Sun. Thus, one can use a Taylor expansion around $r = 0.936$ and write

$$\phi'(r) = \phi'(r = 0.936) + \left. \frac{d\phi'}{dr} \right|_{0.936} (r - 0.936) + \left. \frac{d^2\phi'}{dr^2} \right|_{0.936} \frac{(r - 0.936)^2}{2!} + \dots \quad (32)$$

where $d\phi'/dr$ is determined from eq. (31) by substituting for P the survival probability of ${}^8\text{B}$ neutrinos. However, we neglect quadratic and higher order terms in the Taylor expansion consistent with the approximation used in the derivation of eq. (17).

Finally, we study the effect of twisting magnetic fields on the detection rates in the chlorine, Kamiokande and the gallium experiments. These experiments have different energy thresholds for detection and are, thus, sensitive to different components of the solar neutrino spectrum.

The lowest energy pp neutrinos account for about 54% of the total neutrino signal in the gallium detectors while the contribution of the intermediate energy neutrinos, viz. Be, pep and CNO neutrinos is about 35% and the high energy neutrinos account for another 11%. Thus

$$R_G = 0.54P_L + 0.35P_I + 0.11P_H, \quad (33)$$

where P_L, P_I and P_H are the survival probabilities for low, intermediate and high energy neutrinos respectively. Kamiokande, on the other hand, detects only ${}^8\text{B}$ neutrinos via weak charged and neutral current interaction in the neutrino–electron scattering. In this experiment, electron neutrinos can interact with the water Cerenkov detector via the neutral as well as charged weak currents whereas ν_μ, ν_τ can only interact via the neutral currents for which the cross-section is only about 14% of the total so that

$$R_K = 0.14 + 0.86P_H. \quad (34)$$

Finally, in the absence of any suppression mechanism, intermediate energy neutrinos account for 22% of the neutrino signal in Homestake and high energy neutrinos account for the remaining 78% so that

$$R_H = 0.22P_I + 0.78P_H. \quad (35)$$

The probabilities P_L, P_I and P_H can be calculated from eq. (17) for the respective categories of neutrinos. We take $\mu = 1.5 \times 10^{-11} \mu_B$ and the Akhmedov distribution [20] for the magnetic field in the solar interior. The average energy of low, intermediate and high energy neutrinos are chosen to be 0.420 MeV, 0.862 MeV and 10 MeV respectively. The twisting profile for the intermediate energy neutrinos is given by eq. (28) and by eq. (32) for high energy neutrinos. The low energy neutrinos undergo RSFP conversion in the radiation zone and, thus, are not subjected to twisting magnetic fields.

The detection rates for the three experiments have been depicted in figure 7 for positively twisted magnetic field and in figure 8 for negatively twisted magnetic field. The detection

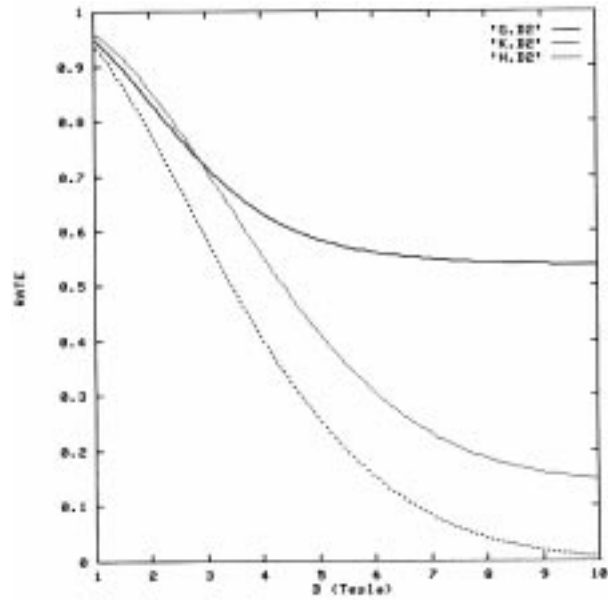


Figure 7. Variation of the detection rates with the solar magnetic activity for positively twisted magnetic field in the solar convective zone for gallium (G), Kamiokande (K) and Homestake (H) experiments.

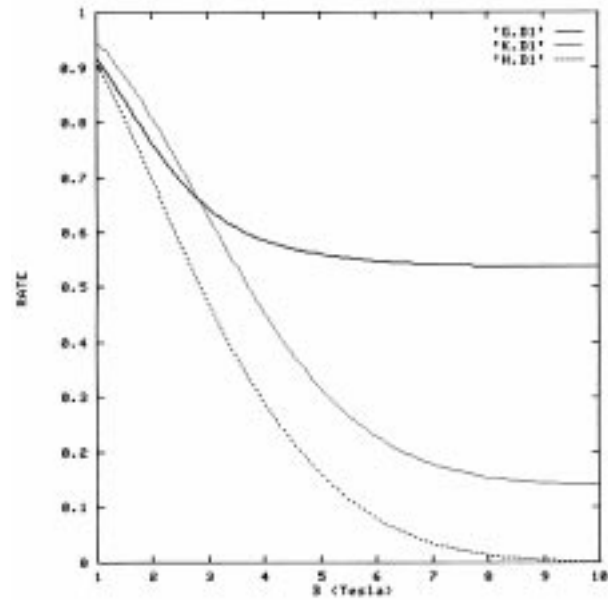


Figure 8. Variation of the detection rates with the solar magnetic activity for negatively twisted magnetic field in the solar convective zone for gallium (G), Kamiokande (K) and Homestake (H) experiments.

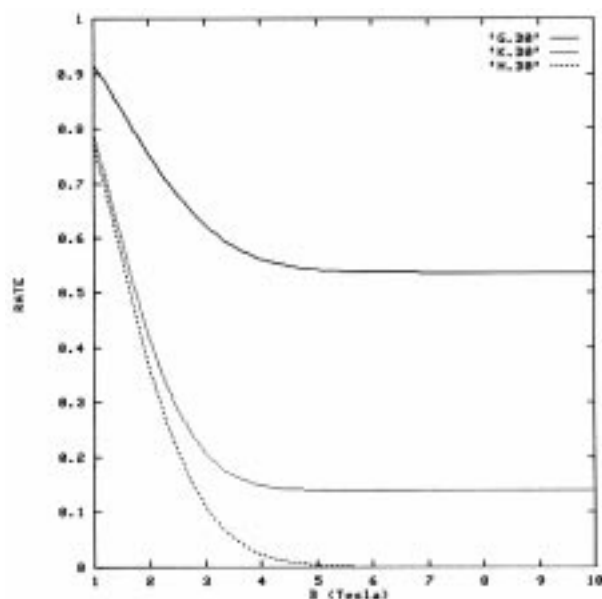


Figure 9. Variation of the detection rates with the solar magnetic activity in the absence of twisting for gallium (G), Kamiokande (K) and Homestake (H) experiments.

rates in the absence of twisting have been depicted in figure 9 for comparison. It is clear from figures 7, 8, 9 that the anticorrelation is expected to be more pronounced in the Homestake experiment. In fact, the gallium neutrino signal is expected to be almost constant in time in agreement with the observations. Also, the presence of twisting (positive as well as negative) reduces the degree of anticorrelation in comparison with the no-twisting scenario (figure 9). However, the anticorrelation is expected to be stronger for neutrinos emerging from the solar hemisphere with negatively twisted magnetic fields, i.e. the southern hemisphere in agreement with the conclusions of Massetti and Storini [21] and Stanev [22] who found that the anticorrelation between Homestake signal and the green corona line to be much stronger for neutrinos emitted in the southern solar hemisphere than for those emitted in the northern solar hemisphere. Preliminary results of this investigation have been reported elsewhere [23].

4. Conclusions

In this work, the resonant spin-flavor precession of neutrinos in twisting solar magnetic fields has been confronted with the solar neutrino observations from various ongoing experiments. Specifically, the anticorrelation apparent in the Homestake solar neutrino data has been taken seriously to derive constraints on the $(\Delta m^2, \phi')$ parameter space and the possible twisting profiles of solar magnetic fields. It is found that a maximum constant positive twisting rate $\phi' \sim 0.9253$ rev/Rs is consistent with the anticorrelation observed in Homestake which is in fairly good agreement with the astrophysical bound on ϕ' : $\phi' \sim 1$ rev/Rs. A constant negative twisting rate in the range $-0.29 < \phi' < -0.21$ rev/Rs is also consistent

with the anticorrelation apparent in the Homestake experiment. However, constant positive twisting rates in reasonably good agreement with the astrophysical bound are possible only for a very limited range of values for Δm^2 : $1.54 \times 10^{-8} \text{ eV}^2 < \Delta m^2 < 1.93 \times 10^{-8} \text{ eV}^2$. The more realistic case of magnetic field with varying twisting rates has also been considered and the twisting profiles in the resonance regions for ${}^7\text{Be}$ and ${}^8\text{B}$ neutrinos have been derived. These twisting profiles have been used to calculate the detection rates for the Homestake, Kamiokande and the gallium experiments with varying solar magnetic activity. It is found that the presence of twisting reduces the degree of anticorrelation in all the solar neutrino experiments. However, the anticorrelation in the Homestake experiment is expected to be more pronounced in this scenario in comparison with the other experiments. Thus the fact that only Homestake has reported an anticorrelation of solar neutrino flux with the solar magnetic activity comes as no surprise in this scenario. Moreover, the anticorrelation of solar neutrino flux in the southern solar hemisphere is expected to be stronger than that for neutrinos emerging from the northern solar hemisphere. This explains in a natural manner the results of the statistical studies of the Homestake data by Massetti and Storini [21] and by Stanev [22] who found that the anticorrelation of the solar neutrino flux with the green corona line (used as an indicator of the solar magnetic activity) is much stronger for neutrinos emerging from the southern solar hemisphere than for those emerging from the northern solar hemisphere. However, at present, the time-variations reported by Homestake are, rather, controversial because of its poor statistics. Hopefully, the next generation high statistics solar neutrino experiments will finally settle the matter.

References

- [1] H Yoshimura, *Astrophys. J.* **178**, 863 (1972); *Astrophys. J. Suppl. Ser.* **29**, 467 (1975); **52**, 363 (1983)
Y Nakagawa, in *Solar magnetic fields* edited by R Howard (Springer Verlag, 1971)
- [2] J D Jackson, *Classical electrodynamics*, 2nd edition (Wiley, New York, 1975) ch. 10
- [3] E Kh Akhmedov, invited talk at the 4th International Solar Neutrino Conference, Heidelberg, April 1997, Report No. IC/97/49.
- [4] C S Lim and W J Marciano, *Phys. Rev.* **D37**, 1368 (1988)
E Kh Akhmedov, *Phys. Lett.* **B213**, 64 (1988)
- [5] B C Chauhan, U C Pandey and S Dev, *Phys. Rev.* **D59**, 083002 (1999)
- [6] B C Chauhan, U C Pandey and S Dev, *Mod. Phys. Lett.* **A13**, 1163 (1998)
- [7] M V Berry, *Proc. R. Soc. (London)* **A392**, 45 (1984)
- [8] J Vidal and J Wudka, *Phys. Lett.* **B249**, 473 (1990)
- [9] A Yu Smirnov, *JETP* **53**, 280 (1990); *Phys. Lett.* **B260**, 161 (1991)
- [10] C Aneziris and J Schechter, *Int. J. Mod. Phys.* **A6**, 2375 (1991)
- [11] S Toshev, *Phys. Lett.* **B271**, 179 (1991)
- [12] A Yu Smirnov, in *Proc. Lepton Photon Symposium and European High Energy Physics Conference, Geneva, 1991* edited by S Hegarty, K Potter and E Quereigh (World Scientific, Singapore, 1992) p. 698
- [13] E Kh Akhmedov, P I Krastev and A Yu Smirnov, *Phys. Rev.* **D48**, 2167 (1993)
- [14] T Kubota, T Kurimoto, M Ogura and E Takasugi, *Phys. Lett.* **B292**, 195 (1992)
- [15] T Kubota, T Kurimoto and E Takasugi, *Phys. Rev.* **D49**, 2462 (1994)
- [16] A B Balantekin and F Loreti, *Phys. Rev.* **D48**, 5496 (1993)
- [17] S Toshev, Talk presented at the *XIIth Moriond Workshop on Massive Neutrinos and Tests of Fundamental Symmetries*, LPTB 92-5 (Les Arcs, Savoie-France, 1992)

RSFP constraints on the neutrino parameters

- [18] E Kh Akhmedov, P I Krastev and A Yu Smirnov, *Z. Phys.* **C52**, 701 (1991)
- [19] J Pulido, *Phys. Rev.* **D48**, 1492 (1993)
- [20] E Kh Akhmedov and O V Bychuk, *Sov. Phys. JETP* **68**, 250 (1989)
- [21] S Massetti and M Storini, *Astrophys. J.* **472**, 827 (1996)
- [22] T Stanev, in *Proc. 4th Int. Topical Workshop on New Trends in Solar Neutrino Physics* edited by V Berezinsky and G Fiorentini (Gran Sasso, Italy, 1996) p. 141
- [23] U C Pandey, B C Chauhan and S Dev, *Mod. Phys. Lett.* **A13**, 3201 (1998)